Danger assessment of the partial discharges temporal evolution on a polluted insulator using UHF measurement and deep learning

Luis Orellana [a], Jorge Ardila-Rey [b,*], Gonzalo Avaria [c,d], Sergio Davis [d,e]

[a] *Karlsruhe Institute of Technology (KIT), Institute for Pulsed Power and Microwave Technology (IHM), Hermann-von-Helmholtz-Platz 1, Eggenstein-Leopoldshafen, 76344, Germany*

[b] *Departamento de Ingenieria Electrica, Universidad Tecnica Federico Santa Maria, Av. Vicuña Mackenna 3939, Santiago, 8940000, Chile*

[c] *Departamento de Fisica, Universidad Tecnica Federico Santa Maria, Av. Vicuña Mackenna 3939, Santiago, 8940000, Chile*

[d] *Research Center on the Intersection in Plasma Physics, Matter and Complexity (P^2mc), Comision Chilena de Energia Nuclear, Av. Nueva Bilbao 12501, Santiago, 7600713, Chile*

[e] *Departamento de Ciencias Físicas, Facultad de Ciencias Exactas, Universidad Andres Bello, Republica 220, Santiago, 8370035, Chile*

ABSTRACT

Pollution over insulators surfaces in outdoor environments is detrimental for long term operation of power systems. The temporal evolution of measurement signals as the contamination increases has not been given much attention. This work proposes presented the analysis of the time series of partial discharges measured with an antenna in an increasing pollution condition until flashover, using a deep learning algorithm in order to identify the early signs of an incoming flashover. Flashover was produced by gradually increasing pollution over a bushing insulator to carry out a binary classification of signals as low or high danger. Different time thresholds were tested and it was concluded that partial discharges measured with antennas can be used as early detection of flashover, and a time threshold at the 70% of total experiment time gave the best result, being noticeable transition from low to high danger signals before flashover.

1. Introduction

Insulators are basic and critical components of high voltage equipment, power transmission and distribution networks, as they withstand mechanical and electrical stresses under high voltage regimes. Since usually those networks operate in outdoor environment the occurrence of flashover due to accumulated pollution in the surface of an insulator represents an earth fault that, depending on its severity, may harm the high voltage equipment itself and compromise the entire operation of the network. Hence, monitoring the pollution in insulators is critical for preventing network permanent damage. Predicting flashover is challenging as the electrical discharge activity is of stochastic nature and it is influenced by environment factors, electrical stress and the presence of different types of pollution. Technical taskforces had worked in recommendations on the topic of contaminated insulators and how to monitor them (33.04.01, CIGRE TF, 2000; 33.04.03, 1994). As stated by Wilkins (Wilkins, 1969), in presence of environmental conditions such as humidity, dew or fog, a contaminated insulator exhibits resistive surface leakage current which is significantly higher to the capacitive leakage current under normal dry conditions. The electrical field distribution is distorted by this phenomena, which is responsible for leading into a full gas discharge over the surface of the

insulator or flashover. In particular, water droplets suspended between the sheds or water patches on the insulator surface contribute to the electrical field distortion and thus the performance of the insulator under flashover (El-Kishky and Gorur, 1996). Considering different electrical field distortions and environmental factors, the conductivity of the pollution layer is the main factor that determines the flashover occurrence as reported by Jin et al. (2021). Because conductivity is related to humidity, when polluted conditions are present, arc discharge activity varies depending on the insulator surface material. Hydrophobic materials, such as polymer insulators, perform better than porcelain ones (He and Gorur, 2016b).

Different approaches have been taken to evaluate pollution severity on insulators in order to select better material or to monitor and plan maintenance. The most straightforward approaches are equivalent salt deposit density (ESDD) and non-soluble deposit density (NSDD) (IEC, 2014), which require direct sampling of the surface's pollution in order to determine the surface conductivity. These are not practical for on-line monitoring as the handling of the insulator itself is required for the measurement. An alternative is the measurement of the leakage current which does not require direct contact with the insulator, but a measurement of current to ground. Different classifications of pollution severity have been reported using this measurement technique (De Santos and

---

Sanz Bobi, 2020; Liu et al., 2016; Zhao et al., 2015; Richards et al., 2003; Chandrasekar et al., 2010). Non-contact measurements consider from the characterization of acoustic waves, to the measurement of different wavelengths in the electromagnetic spectrum. As acoustic sensors can detect ultrasound coming from the arc activity in polluted insulators, they were used to measure and classify partial discharges in outdoor insulators in Ferreira et al. (2012) and Polisetty et al. (2019). RF antennas can also detect the electromagnetic waves that come from the surface partial discharge activity in polluted insulators without the need of close connection to the sensor: in Shurrab et al. (2013) antennas were used to monitor and classify partial discharges on insulators and in Paula Santos Petri et al. (2020) they were used for developing a portable monitoring system. Optical measurements can detect infrared emission due to heating associated with the arc activity (Reddy and Nagabhushana, 2003; Jin and Zhang, 2015), in the visible spectrum they can detect pollution by image recognition (Mussina et al., 2020; Jin et al., 2017), and ultraviolet measurements can also detect arc activity (Jin and Zhang, 2015), or combinations of all these optical measurements (Jin et al., 2017). A comparison and combination of the techniques, from acoustic, antenna, leakage current and optical measurements, can be found in Bezerra et al. (2009).

A large number of diverse signals and images are obtained using the measurement methods cited above, and machine learning algorithms are used to find patterns in the data, aiming to interpret and classify them in terms of some degree of pollution severity. Deep learning approaches have been shown to be most useful in classifying the measurements (Shurrab et al., 2013; Polisetty et al., 2019; Paula Santos Petri et al., 2020; Mussina et al., 2020). Machine learning methods are practical to solve these classification problems in an automated manner and recent state of the art reviews have been published (Lu et al., 2020; El-Hag, 2021).

Even before flashover, the same conditions that allow its occurrence can produce surface partial discharge, therefore arising the question as to how the arc activity evolves over time under contamination conditions. The detection partial discharges is the backbone of most of the non-contact measurement methods cited above. The contribution of the present work is to demonstrate that time evolution of signals from partial discharges measured with an antenna can be used to detect changes on the signals from low to high danger of flashover. An example of this type of forecast using deep learning neural network (long short-term memory layers) is informed in Kates-Harbeck et al. (2019), where the onset of fusion plasma disruptions in experimental reactors was tested. Such architecture could help to interpret the time of evolution of the partial discharges from no activity until flashover in an analogous manner.

Experiments were conducted to reproduce the electrical discharges, both partial and flashover, on a fully salt polluted bushing insulator from a dry condition, i.e., no discharges, to a highly wet, and thus conductive condition, that produced the final flashover. An open slot antenna, tuned in the ultra-high frequency range (UHF), measured the electromagnetic bursts from the surface and flashover discharges. During the measurement, rated ac voltage was applied to the polluted insulator while short bursts of saline water were sprayed periodically, increasing surface partial discharge activity until flashover occurred. Then a deep learning neural network, consisting of convolution layers for feature extraction and long short-term memory (LSTM) cells for sequence interpretation was used to classify the time series of antenna signals in terms of different time thresholds. The signals before a given threshold were assigned as class 0, interpreted as low danger of flashover, and those after the threshold were assigned as class 1, interpreted as high danger of flashover. The approach using different time thresholds allowed to interpret how early a reasonably dangerous partial discharge activity can be recognized from experimental data.

The paper structure is as follows: Section 2 describes the experimental set up to replicate the increasing pollution on an insulator. Section 3 details the time series of antenna signals measured, the proposed analysis, and the deep learning algorithm utilized. Section 4 includes the results of the model for different analysis conditions and its discussion. Finally, Section 5 presents the conclusions.

2. Experimental methodology

The experiment runs were planned to measure the insulator's surface partial discharge activity at distance, by means of an antenna, from a dry salt polluted initial condition, with no detectable discharges, until flashover due to a critical conductivity because of the humidity . This form of contamination allowed for a gradual increase in the salt deposit on the surface of the insulator, simulating what happens in numerous insulators over time, where contaminating agents accumulate on the surface. It should be noted that in a real situation, this process may depend on different factors and the evolution from a certain condition to a possible flashover may occur through various paths. The electrical circuit of the experimental configuration is shown in Fig. 1. The test circuit consisted of a high voltage transformer 400 V/150 kV, where energy supply was taken from a 220 V 50 Hz power grid, controlled by means of a regulating transformer. A capacitive voltage divider was used in parallel to the test object in order to measure the applied voltage. The test object was a transformer bushing insulator made of porcelain, rated 34.5 kV with 12 sheds. The porcelain insulator was chosen because it is mainly found in primary equipment such as power transformers and is known for its poor performance, thus being more critical in polluted environments compared to hydrophobic materials (He and Gorur, 2016b), such as polymer.

The insulator was sprayed before each test run with a saline pollution consisting of 167 gr/Lt of Na–Cl dissolved in water and then dried with an industrial dryer to produce an initial salt deposit on the surface. An example of an initially polluted insulator is shown in Fig. 1. During each test run nominal 34.5 kV was applied to the insulator until the end of the experiment, while every three or five minutes salt pollution was sprayed with a short burst of about 1–2 s, using a manual spray bomb to increase the humidity of the polluted insulator. For each measurement run, the same insulator model was used, because it was observed that at the end of each experiment run the insulator did not have visible damage on its surface as a result of flashover. Likewise, the insulator was properly cleaned and dried before starting the next measurement process. Since an antenna was used as sensor, manual sprays were preferred over electrical controlled sprays, as the former allowed no additional electromagnetic (EM) noise to be acquired during the measurements. To contain the salt pollution, the insulator was enclosed in an acrylic cage, see Fig. 1. On top of it was placed a light bulb to dry the salt pollution sprayed to the insulator, thus reproducing the effect of accumulated pollution.

In each test run, signals were recorded first using a low trigger, specifically 15 mV, just above background level to obtain some background or low amplitude partial discharges, since no high amplitude signals were observed at the beginning with a dry condition. After this initial signals acquisition, the trigger was increased to the value of 25 mV and held until the end. The acquisition of signals above background noise started with the periodical manual sprays and lasted until the appearance of continuous flashover, thus ending the test run.

The diagnostic signal was the electromagnetic burst from surface partial discharges and flashovers, detected with a commercial directional open slot antenna (KC R102 Deepace), see Fig. 2a, with dimensions of 12.0 cm × 16.9 cm and thickness of 1 mm, and a SMA female connector as output port. Open slot antennas such as Vivaldi have been reported to successfully classify partial discharges discarding external sources of EM noise in the radiofrequency spectrum and directional property (Robles et al., 2013). A MS2035B vector network analyzer was used to measure the reflection response or S_{11} parameter, critical to describe the frequencies for which an antenna is tuned and those diminished, resulting in a good response, indicated by lowest values of reflection coefficient, mostly concentrated above 1500 MHz, with valleys at approximately 1500 MHz and 2500 MHz, see Fig. 2b. The
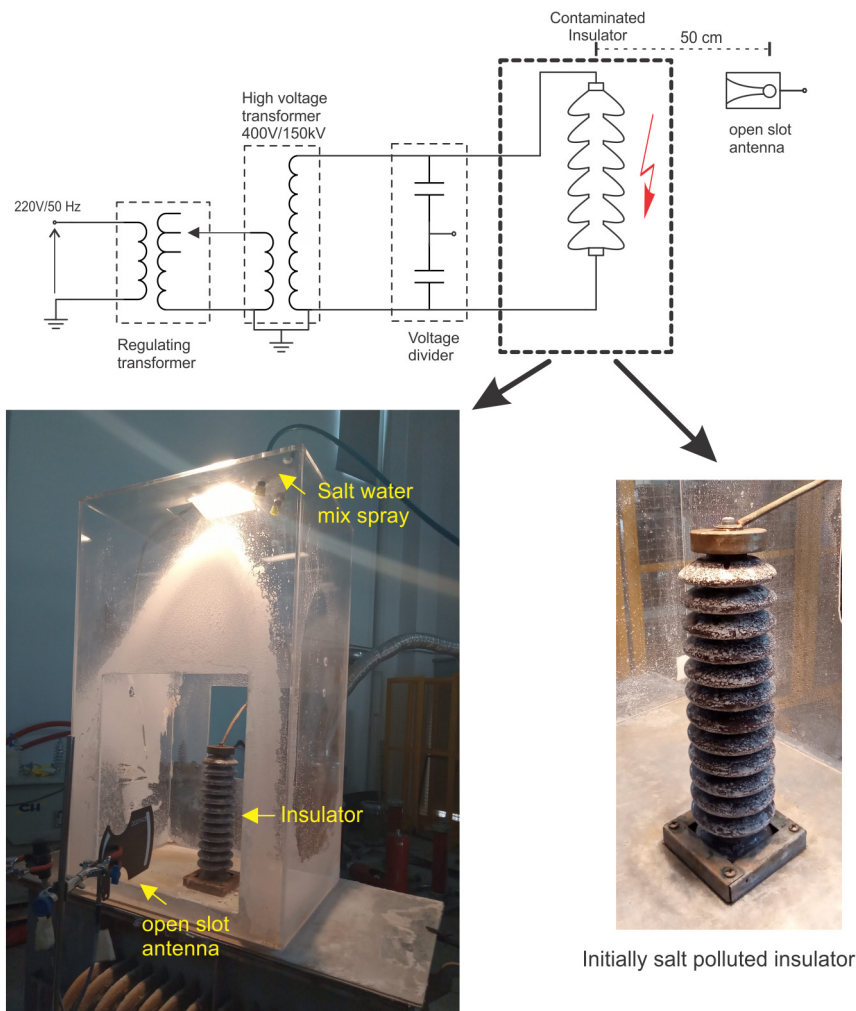
Fig. 1. Electrical circuit, experimental setup, and a salt polluted insulator before starting test runs.
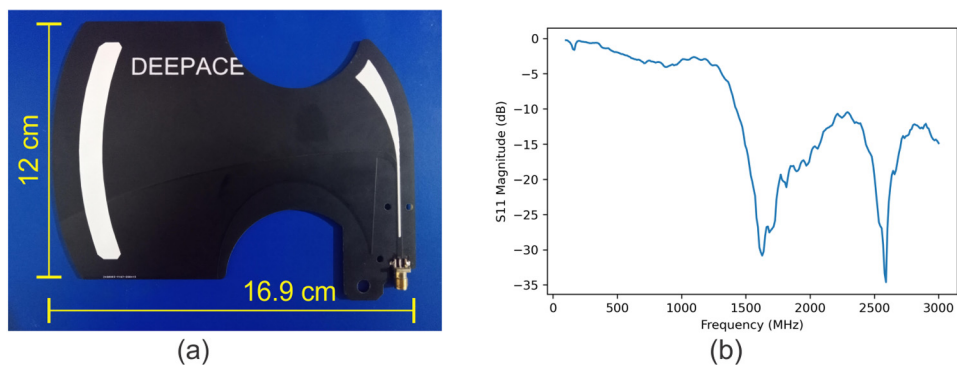

Fig. 2. (a) Antenna and (b) S11 response.

antenna was placed at a distance of 50 cm from the insulator, see Fig. 1. Because of its directional property it was pointed to the expected source of EM waves, i.e., the polluted insulator. The signals were recorded using a Keysight Infiniium DSOS804a oscilloscope using a time window of 1 μs and sampling frequency of 5 GS/s, thus having 5000 points per signal. This setting was more than enough to register the pulses associated with partial discharges detection, as for the tuned frequencies of the antenna the transient signals spanned for at most hundred nanoseconds.

3. Experimental data and proposed analysis

3.1. Model description

The aim was to determine when the partial discharges activity evolves to become dangerous and a predecessor of the flashover. It is a complex task to identify if a partial discharge activity is dangerous or not because the diverse measured signals are not uniformly distributed in time. To tackle this challenge the time series of partial discharges signals were analyzed as a binary classification in terms of time, using a deep learning model that combined the extraction of
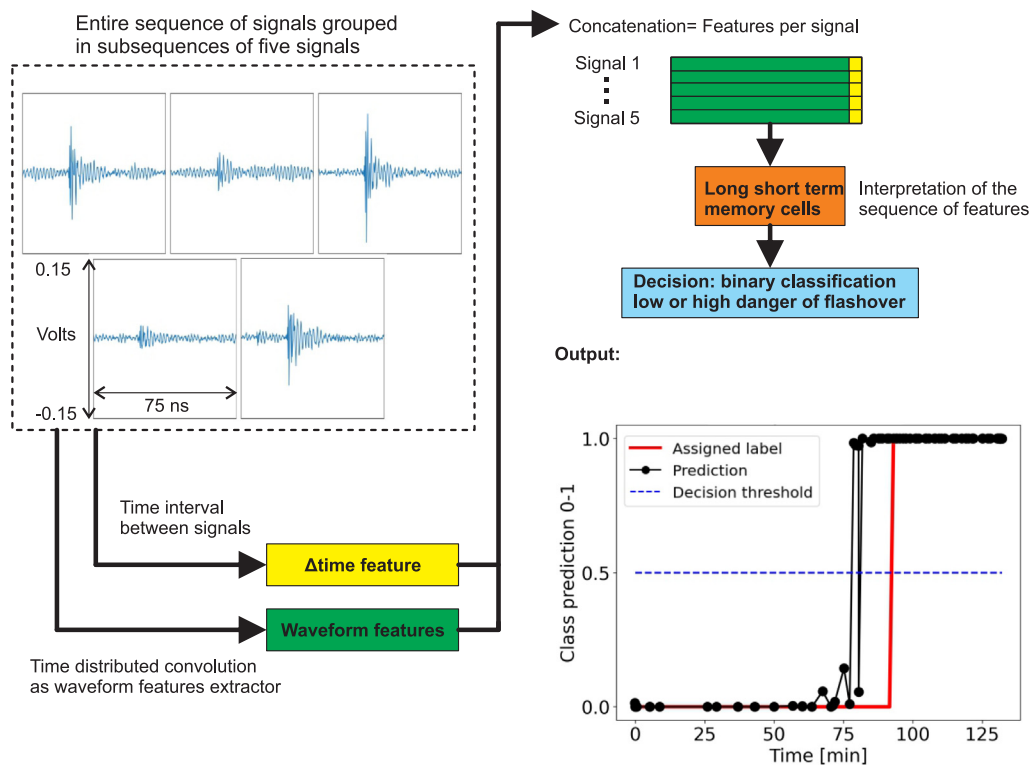
Fig. 3. Analysis scheme.

features from the signals waveform, the time difference between two consecutive signals, and the sequence interpretation of those merged features. This approach showed good results in other physical phenomena forecast (Kates-Harbeck et al., 2019). The binary classification was carried out with a supervised learning approach. The model was trained to identify the partial discharges activity as low danger of flashover, class 0, and high danger of flashover, class 1. Low danger being the signals at the very beginning of the experiment and high danger those close to the moment of flashover. Different points in time, named time thresholds from now on, were tested to make this separation of classes. By changing these time thresholds, the idea was to find a model output that balances no early class 1 classification (false positive too early) and clear transition to class 1, preferably before flashover. In this manner the model output inferred the coming flashover.

To analyze the signals and after different trials, the approach that used the sequence interpretation of both waveform features and their time interval between signals, i.e., a measure of how often the discharges were detected, produced better results than, for instance, just using the waveform characteristics. The model extracted the waveform's features via convolution layers and concatenated them with the time interval between signals, and then the sequence of those features was processed with long short-term memory cells. Convolutional layers had been used extensively in areas such as image recognition, in particular in the area of partial discharges activity recognition (Paula Santos Petri et al., 2020; Mussina et al., 2020; Lu et al., 2020). A model based on convolution and long short-term memory (LSTM) cells was reported to successfully forecast physical phenomena (Kates-Harbeck et al., 2019). To use these memory cells, data was separated in time steps or groups. Also, grouping signals, takes into consideration the behavior of the entire group of signals features rather than their individual features, hence reducing the influence of sporadic signals that can be, for example, related to strong electromagnetic noise from electronic equipment or the arc activity itself, given the randomness of the phenomena, which can be of high amplitude, but not necessarily dangerous if it is not frequent in time. Fig. 3 illustrates the analysis carried out and at the bottom of the figure an example of the results

obtained is shown. The output of the model is a binary classification decision that is made for each group of signals that conform each experiment run (black line). The assigned label of the groups (red line) was according to a given time threshold. The time point when the partial discharge activity evolved to become dangerous can be determined when the classifications start to appear with probability above a certain decision threshold (blue line), 0.5 for example.

3.2. Experimental data

From the experimental setup described in the previous section, ten experiment runs were made. Each run corresponds to a sequence of antenna signals gathered during the contamination process. In Table 1 are summarized the number of signals obtained in each run and their respective time duration (from dry condition to flashover). Experiment runs lasted between one to four hours. This time depended mainly on the quantity of the initial salt deposit and frequency of salt water sprays. In experiments 1 to 5 the salt sprays were applied each 5 min, in experiments 6 to 10 they were applied each 3 min. These time intervals between sprays were chosen to give time for the wet process, i.e., the droplets flowing down the insulator, to slowly generate a partial discharge activity, that in early stages of the experiment started with a few discharges and then ceased because the humidity dried off. In later stages, the partial discharge activity is sustained in time until the flashover occurred. On the contrary, a constant spray of salt pollution would have produced almost immediate flashover with no chance of effectively observe how the arc discharges appeared as the wetting process took place. The spray frequency partly explains the diverse experiment times obtained. It should be noted that the number of signals obtained in each run is not necessarily correlated with the experiment time because the process itself is highly stochastic and the sprays were manually controlled, so even one second of additional pulsation implied more salt droplets flowing down the insulator and thus more discharges were produced. In addition, following the first continuous flashover observed, a strong humming sound was audible, therefore frequent signals were detected by the antenna, increasing
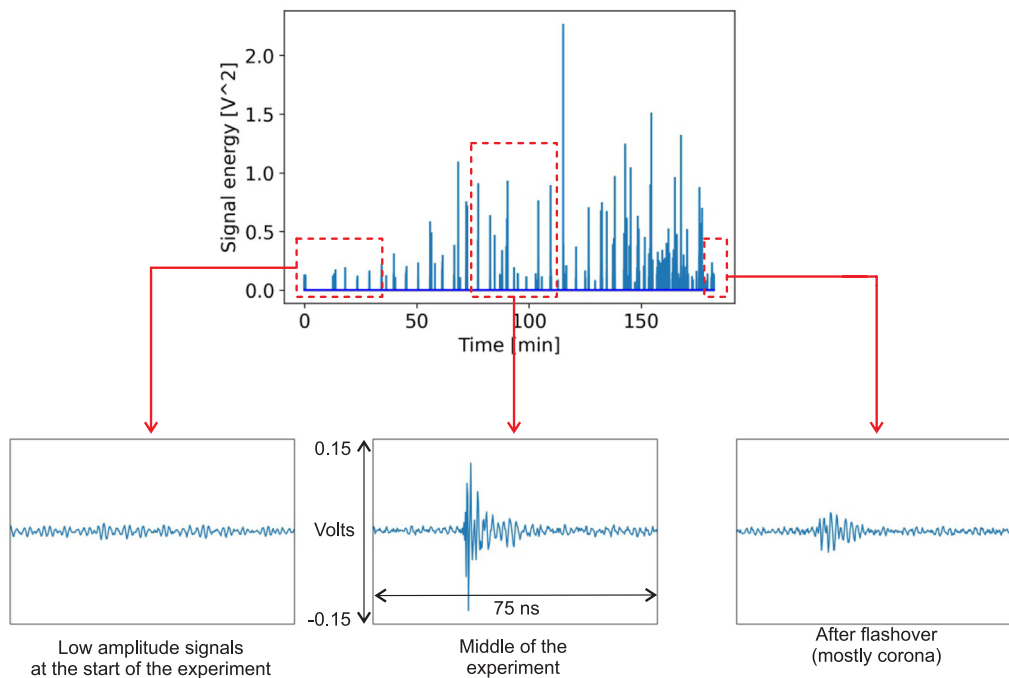
Fig. 4. Example of experiment run and signals.

Table 1
Experiment runs details.

Experiment	Number of signals	Experiment time [min]
1	1565	182.45
2	985	100.45
3	2745	205.87
4	2775	237.13
5	2220	122.22
6	1430	132.13
7	1395	136.63
8	1535	168.07
9	1160	126.65
10	1645	70.70

the number of signals acquired at the end of the experiments in an uncontrolled manner. In some runs, in particular the experiment 10, it was observed that salt water droplets suspended between the insulator's sheds, tended to produce more partial discharge activity, thus more signals were acquired, even though it was the shortest experiment run obtained.

To illustrate the sequence of signals of an experiment run, Fig. 4 shows the sequence of the signals' energy, which is a feature parameter used to describe partial discharges detected by antennas Reid et al. (2012). Energy is calculated as $\sum_{i=0}^{N} v[i]^2$, where $v[i]$ are the samples of a given signal having a total of N points (5000 points in the measured signals). The sequences obtained can be described as follows: first not so high amplitude and not frequent partial discharges at the start, then moderate to high magnitude and more frequent partial discharges during the middle of the experiment, and finally, near flashover and afterwards a mix between high magnitude and even corona partial discharges with high repetition rate. This time behavior of the partial discharges sequence is more or less similar for all the experiment runs, mainly because the experiment procedure of salt accumulation and increasing of humidity was the same, but given the stochastic nature of the phenomenon they span different total experiment times.

3.3. Proposed analysis

As all experiment runs ended with a sustained flashover, the aim was to determine when the partial discharge activity clearly evolved to

become dangerous, i.e., predecessor of flashover. To interpret the time evolution of partial discharges a deep learning model with memory layers was implemented to analyze the data and classify the signals as low or high danger of flashover. As the exact or correct label of such signals classification it is unknown a priori given the diverse signals measured from the phenomena, it is only known that signals with low danger of flashover are expected to be found at the beginning and signals with high danger of flashover are to be identified at the end of the experiment. If the antenna signals are to be useful at this task then, at sometime during the experiment, the antenna signals behavior must change to reflect this transition from low to high danger of flashover. Thus, the model needed to identify this transition based on just the antenna signals.

In order to use memory layers, signals had to be grouped into subsets of five time steps because this way the model produced reasonably good results in contrast to larger groups. This approach gives more importance to the behavior of a group of signals rather than their particular waveforms, thus reducing the influence of sporadic signals which appeared due to the randomness of the phenomena or another possible external sources of electromagnetic noise. The groups were labeled as class 0 (low danger) or class 1 (high danger) to be analyzed as a binary classification problem carried out with the deep learning model. A time threshold was defined to separate both classes in each experiment dataset, i.e., a point in time when the change of antenna signals behavior should occur: before the threshold the groups of signals were labeled as class 0 and after the threshold, class 1. Eq. (1) shows the label definition where T_{max} is the experiment total time, see Table 1, and $t_{threshold}$ a fraction of total time to define the time threshold.

$$y = \begin{cases} 1 & t >= T_{max} \times t_{Threshold} \\ 0 & \text{Else} \end{cases} \quad (1)$$

Different time thresholds had to be tested in this study because results can differ with different output labels. If the model is trained to learn patterns in the partial discharge activity near flashover it can be found of little use as it would give no much prediction horizon. On the contrary, just at the start of the experiment the problem is trivial as all experiment runs ended with flashover. In a practical application, the time threshold definition might also depend on how critical the
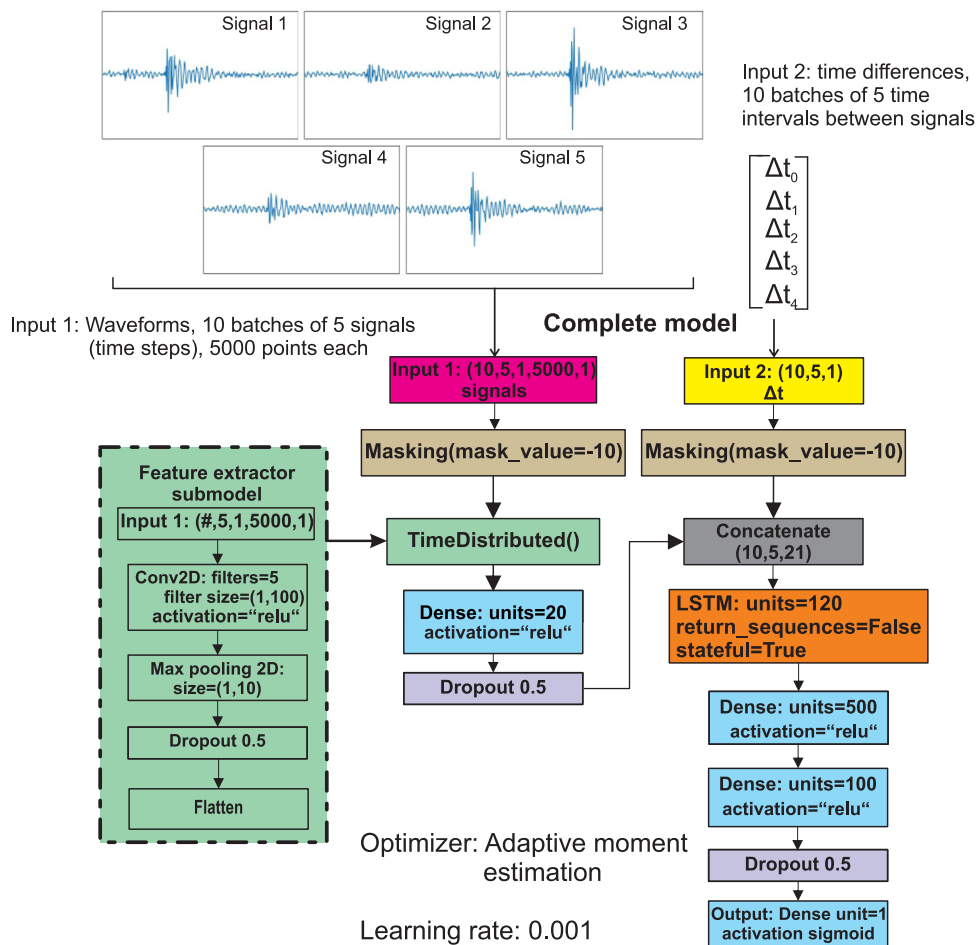
Fig. 5. Neural network model.

equipment under study is, so an early time threshold could be needed for critical equipment while for others it could be relaxed. As most of the signals were detected from about 40% of experiment time onwards, the time thresholds considered were 0.5, 0.6, 0.7, 0.8 and 0.9. Time thresholds below 0.5 produced strong data imbalance between classes, making prediction by mere chance because it would be trivial for the model to just predict the most frequent class 1 to get a good performance score.

In order to achieve generalization, a deep learning model requires many examples for its training, this presents a problem for phenomena that takes too much time to develop, because the available measurements are not enough. Such is the case of the experiments of this study. A balance between feasible experiment time and enough experiment samples had to be reached. A reasonable justification for the number of experiment runs is as follows: Although ten runs were reported, note that each consists of the order of a thousand signals, see Table 1, thus it was considered that enough signals samples were available for binary classification of the deep learning analysis. Also, the number of signals depended on the trigger level. A low value maintained during the whole experiments would have produced a large quantity of signals, mostly background noise, making the data size unmanageable and of little use.

To take the most advantage of the ten experiments, the model was cross validated using the K-folds approach (James et al., 2013). In particular, K = 3 was used, meaning that, at random, two thirds of the runs were used in the training process and the third left was used as testing. The training process was implemented for a maximum of 100 epochs. It was observed that the minimization of the loss function occurred during this number of epochs, and the evaluation of generalization was made based on the test set directly. This process

was repeated until all ten runs were part of the testing subset. It should be noted that in each training/testing separation the model was redefined, therefore a model with new parameters was used in each training/testing iteration. For the main purpose of this work it was more important to obtain consistent binary classifications in terms of time than the model itself. An optimization of this model is beyond the scope of this work as first the usefulness of the measurement signal had to be assessed, i.e., to relate two physical phenomena. Using the K-folds approach and the model redefinition in each iteration, the information of one experimental run learnt by the model during training was not used again when the same run took part of the test subset. The process was repeated for each five time thresholds considered in the analysis.

3.3.1. Deep learning model

As mentioned at the beginning of this section, the proposed model to analyze the data of antenna signals was a combination of convolutional and long–short term memory (*LSTM*) layers: the convolutional part to search for features in the waveforms and the LSTM to interpret the sequence. This model was implemented in the Python programming language using Keras for Tensorflow.

A convolutional layer consists of convolution operations between an image and a filter matrix which passes along every data point of the image. This calculation allows a model to learn local features of an image, such as edges or particular shapes (Lecun et al., 2015). The 5000 points signals acquired with the oscilloscope were interpreted as a 2D matrix with one of its dimensions equal one and the other 5000. It is worth noting that there are several alternative methods to implement feature extractors for a given signal, such as utilizing mathematical transforms (e.g., wavelet), directly reshaping the input waveform to
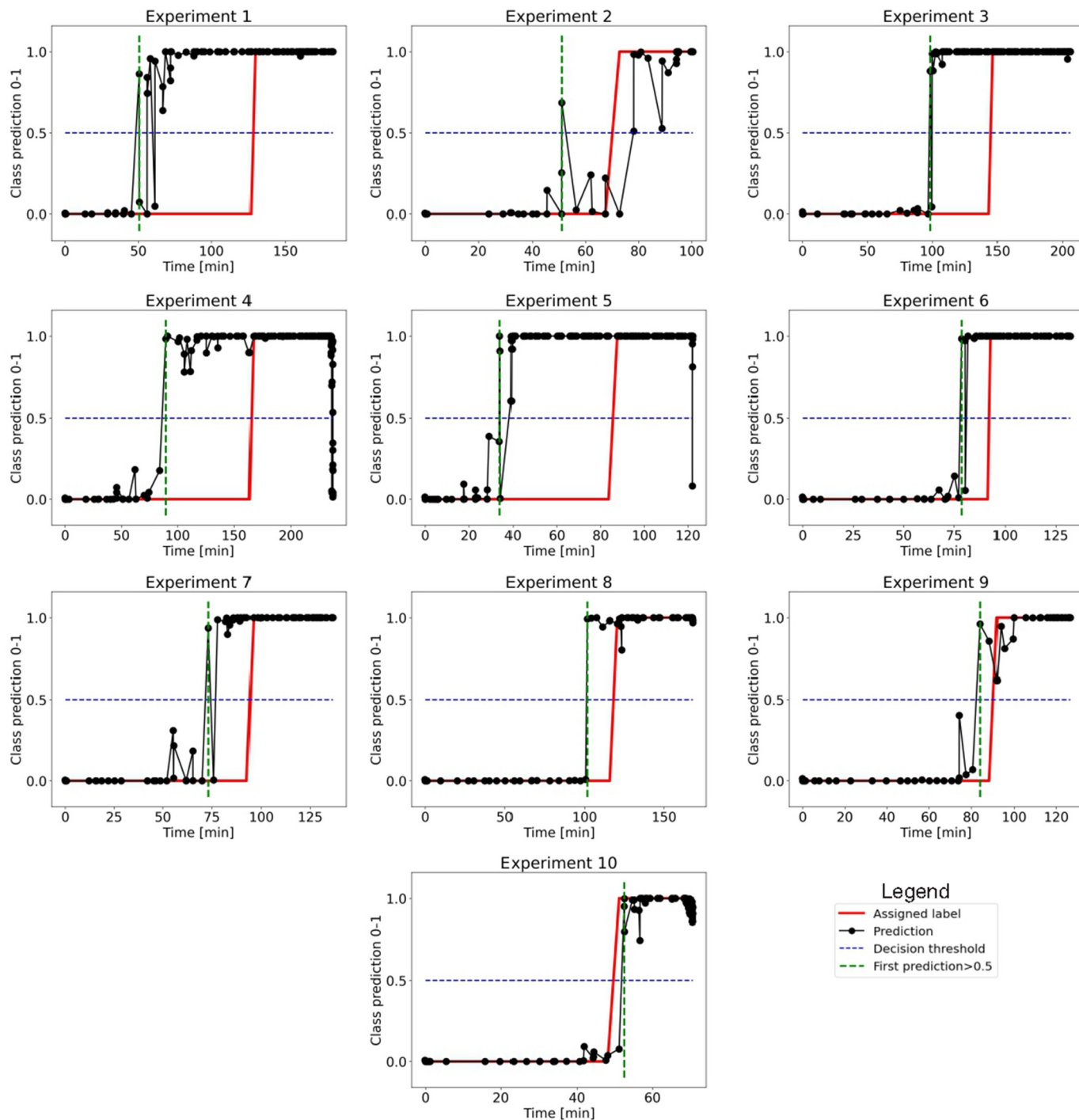
Fig. 6. Results using a time threshold of 0.7.

convert the 1D signal into a 2D matrix, or processing the signal with recurrent layers. In terms of simplicity, convolution can be considered as one of the most practical approaches for implementing this analysis.

The long short-term memory is a recurrent neural network architecture that allows the storage of data representations, i.e., a hidden state, given by recent events and those that are far behind in time (Hochreiter and Schmidhuber, 1997).

The signals gave information about the shape of the pulses associated with the partial discharge detection and the time interval between recorded signals gave information regarding how quickly they occurred. The scheme of the deep learning model to capture these features is summarized in Fig. 5. The feature model extractor obtained

the features of the signals waveforms. This information was interpreted in a time distributed manner in the complete model, meaning that those features were determined for each signal in the group of five. This result was concatenated with the time interval sequence (another feature). The long LSTM layer analyzed the sequences of those concatenated features, and the final decision was made by a dense layer with a single unit and activation function sigmoid as is traditionally used in binary classification. The loss function implemented was binary cross-entropy.

The LSTM layer was implemented as *stateful*, meaning that a fixed number of groups of five signals, i.e., the number of batches, had to be specified for the model to be able to retain memory of the previous behavior in an experimental run data. As shown in Fig. 5 this number

was specified as 10. A too large batch number, for example 100, was considered impractical as the model would need a large number of signals to make a prediction. On the contrary, if the batch number is 1 the classifications were too oscillatory in time, thus useless for the intended aim of this study. The total number of groups of five signals in an experiment run data had to be multiple of 10. Therefore, a padding was applied to the data by adding fictitious signals with only -10 value at the start of each experiment run measured sequence of signals. The padded values were left out of the analysis in the complete model by applying masking layers right after the inputs layers.

4. Results and discussion

In most of the runs, and depending on the time threshold under consideration, the results of the binary classification allowed to make a clear distinction between low danger and high danger groups of signals, although this distinction did not occur as exactly as the proposed label assignation by the time threshold, i.e., the distinction made by the model could occur before or after this time threshold. Also, oscillations in the classifications could be observed for some runs, indicating that the model was unsure of the classification. One of the results considered of interest was the classifications for the time threshold of 0.7 shown in Fig. 6. The description of the curves shown is as follows: the red line is the assigned label to each group of five signals according to the time threshold under study, Eq. (1), the prediction or classification of the model is shown with a black line, and the blue horizontal line corresponds to a decision threshold with the value of 0.5. Also, the vertical green line, which corresponds to the first time the model output goes above the decision threshold is highlighted since that is the class transition expected to find with the antenna signals and the model. The decision threshold is the value set for classification. If the output of the model, a sigmoid, is above this value, it is considered as class 1, if it is below the value, it is class 0. This threshold can be defined with different values depending on how strict the identification of dangerous partial discharges activity needs to be. For a practical monitoring application, at the point in time in which the model output reaches the decision threshold (highlighted with the green vertical line), an alarm would trigger indicating the need of cleaning. The rest of results are in Figs. A.8–A.11 in the annex section Appendix.

The point in time when the first classification of class 1 occurs, was used to define an error in time related to the class labeling proposed. It was devised as a measure of how much time earlier or later the class transition occurs compared to the proposed class labeling. The error, Eq. (2), corresponded to the time difference in minutes between the first time when the model assigned a class probability above 0.5 ($\hat{y} >= 0.5$), though this decision threshold could vary in a practical application depending on how sensitive the decision need to be, and the time when the first class 1 label ($y >= 0.5$) appears according to the time threshold, Eq. (1). The errors obtained are shown in Table 2 and in Fig. 7.

$$\textbf{Error} = t[\hat{y} \geq 0.5]_0 - t[y \geq 0.5]_0 \qquad (2)$$

With time threshold of 0.5 and 0.6 the classifications tended to assign class 1 long before the time threshold, see Figs. A.8 and A.9 and some experiment runs had class 1 classifications right at the start. Since the starting condition of the insulator was highly polluted it could had been possible that with the first sprays the partial discharge activity started in a similar manner to those encountered near the middle of the experiment, so with the time threshold of 0.5 and 0.6 the model learnt to recognize this activity too early. Note that the average and dispersion of the errors in time prediction were greater for time thresholds 0.5 and 0.6, see Fig. 7. For some runs, the model with these thresholds seems to be confused in making a distinction between low and high danger groups of signals, although for others it performed reasonably.

With time thresholds of 0.7, 0.8 and 0.9 the absolute average error and the dispersion were lower. The results of 0.7 and 0.8 thresholds

Table 2
Classification errors, mean and standard deviations, in terms of time thresholds.

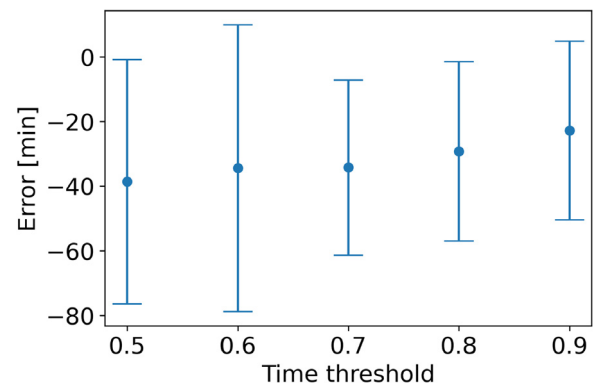|	Errors per time thresholds [min]				
	0.5	0.6	0.7	0.8	0.9
Experiment 1	−93.4	−58.9	−78.9	−60.2	−30.0
Experiment 2	−5.5	−11.0	−21.7	−1.0	8.5
Experiment 3	−44.5	−25.8	−48.2	−57.3	−73.6
Experiment 4	−117.3	−143.2	−77.5	−69.7	−5.8
Experiment 5	−55.3	−73.5	−53.6	−59.6	−62.0
Experiment 6	−10.8	−19.2	−14.3	−14.8	−28.0
Experiment 7	−21.4	−26.8	−22.9	−21.3	−38.9
Experiment 8	−31.2	0.0	−18.9	−13.2	3.8
Experiment 9	−10.5	16.3	−7.9	6.7	10.3
Experiment 10	3.5	−2.5	1.3	−2.0	−12.6
Mean	−38.6	−34.5	−34.3	-29.2	−22.0
Standard deviation	37.8	44.3	27.0	27.7	27.6

Fig. 7. Mean and standard deviation of errors per time threshold under study.

were considered the best since the dispersion and mean error were the lowest, respectively, and the time classifications were reasonable, see Figs. 6 and A.10, in the sense that a clear transition from class 0 to 1 could be observed in most of the runs before or almost at the time threshold used. For the 0.9 threshold, see Fig. A.11, the lowest absolute average error, some runs showed the transition into class 1 considerably after the threshold, almost at the last minutes of the experiment, when the flashover was already happening. The transition occurring after the threshold was interpreted as bad performance because it indicated that no early signs of danger was detected as it was the case of the threshold of 0.9. Also, in a possible application, such extreme limit is not recommended since it has been demonstrated that flashover on service insulators can occur at lower contamination levels than laboratory tests (He and Gorur, 2016a). On average, the transition from class 0 to 1 was observed before the time threshold studied, see the negative mean values of errors in Fig. 7.

It should be noted that given the fixed experimental method focused on contamination accumulation and increasing of humidity, the time evolution of the signals was similar in the experiment runs, so the generalization to other types of contamination procedures is not guaranteed based on these results.

The stochastic nature of the electrical discharges and their appearance in a wet salt polluted environment produced variability in the duration of all the experiments made, despite of the controlled environment and procedure of experiments. Moreover, it is expected that the shape of the insulator could also affect the results, as the salt droplets needs to flow down the insulator to excite the surface partial discharge phenomena, thus producing different flashover test results (He and Gorur, 2016b). Thus, for a practical application, these same experiments should be made with different shape insulators.

Taking into account the different results obtained, it was not possible to determine an exact time from which the flashover could be predicted with total certainty, but the antenna measurement can be
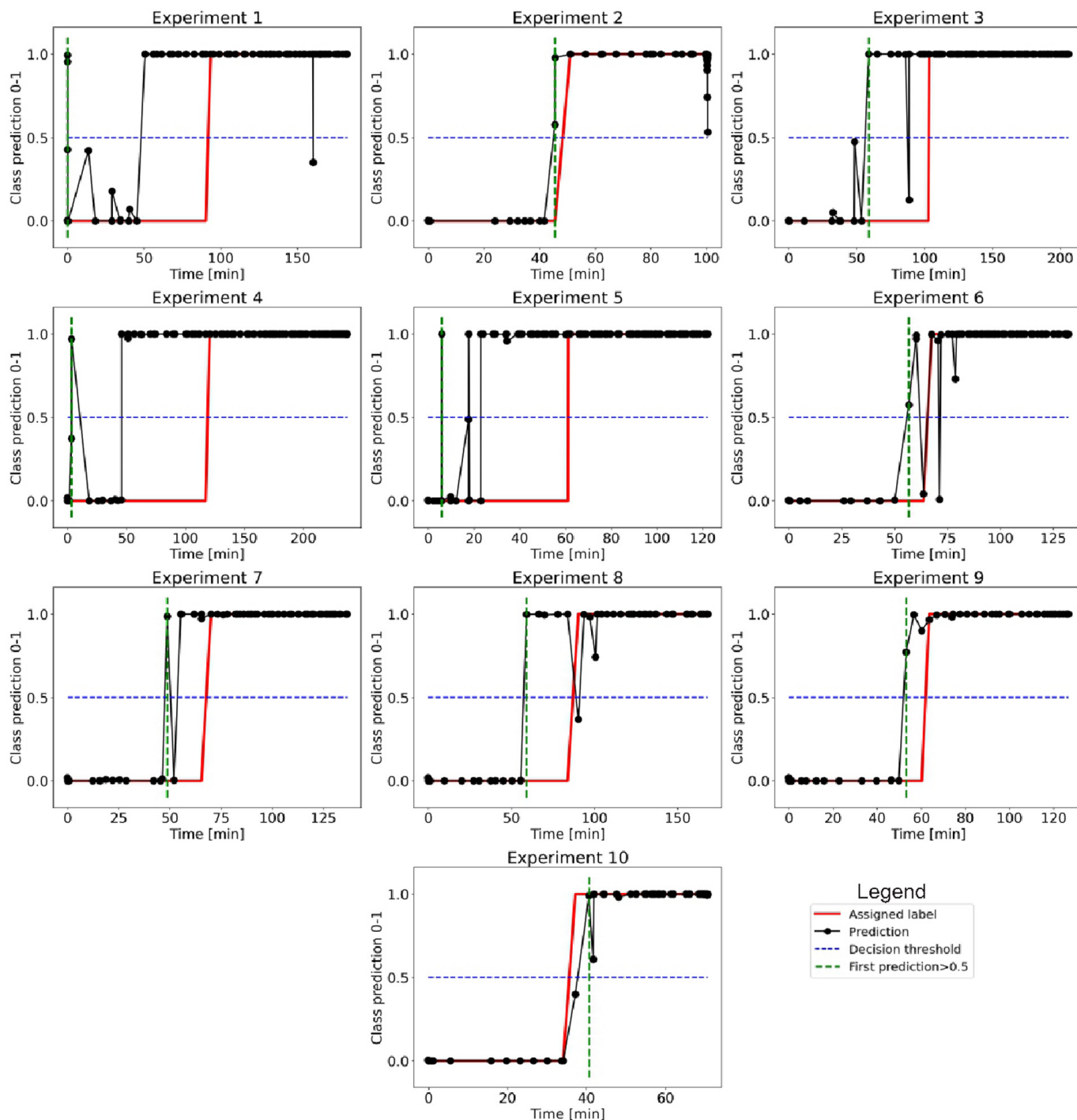
Fig. A.8. Results using a time threshold of 0.5.

in fact used to at least find a behavior that distinguishes a dangerous partial discharge activity and how this evolves in time. A completely negative result would have been to obtain the prediction curve of the oscillatory model for all runs of the experiments and regardless of the time threshold. Therefore, the measurement of partial discharges using an antenna have some information that can be related to a possible future flashover in this particular experimental procedure. The experiment setup and methodology clearly differs from a real on site situation for an insulator, being the application of salt water pollution and relative antenna orientation the most determinant factors in the signals obtained. If the open slot antenna was not directly oriented to the path were the droplets flow, then way less signals would be acquired, thus making this type of measurement less sensible to the phenomena. A future work needs to tackle the optimization of the model, a more sensible antenna and experimental conditions closer to the reality of this phenomena.

5. Conclusions

In this work ten experimental series were analyzed to determine how the partial discharge activity on a salt polluted insulator evolved into flashover as the humidity increased. As this phenomenon is highly stochastic and diverse sets of signals from the partial discharges, were measured at a distance with an antenna, a deep learning approach
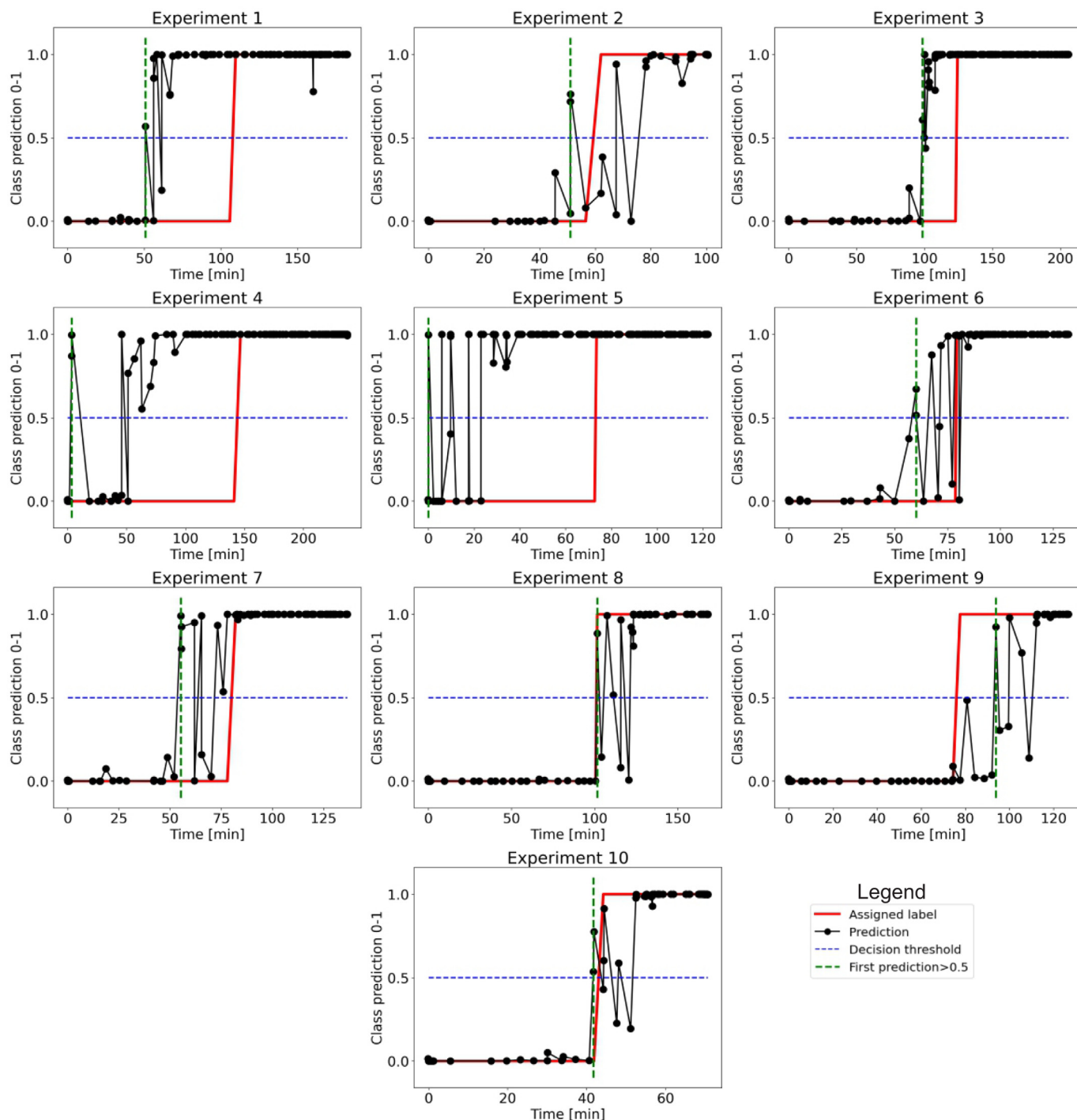
Fig. A.9. Results using a time threshold of 0.6.

with time memory layers was implemented to look for patterns that could be interpreted as indicators of change in partial discharge activity that could lead to flashover. The analysis was carried out as a binary classification where groups of signals were labeled as low danger, class 0, before a certain time threshold, and high danger, class 1, after it. Five different time thresholds were tested in terms of fraction of total experiment time: 0.5, 0.6, 0.7, 0.8 and 0.9.

Using the time thresholds below 0.5, 0.5 and 0.6 resulted in classifications too early as class 1, even as some of the experiments started. With the extreme 0.9 threshold some experiments were labeled as dangerous only right at the occurrence of flashover, thus in some

cases no early signs of dangerous partial discharge activity in the data were found. The best classification performance in terms of time was obtained using the threshold of 0.7 and 0.8. Early signs of dangerous partial discharge activity can be detected early if a deep learning model is trained to classify groups of discharge signals using these thresholds.

It was concluded that the use of an antenna to measure partial discharges allows distinguishing between groups of signals with low or high danger of flashover, with a reasonable time identification between these two classes. However, no certain time to the flashover can be determined by this approach.
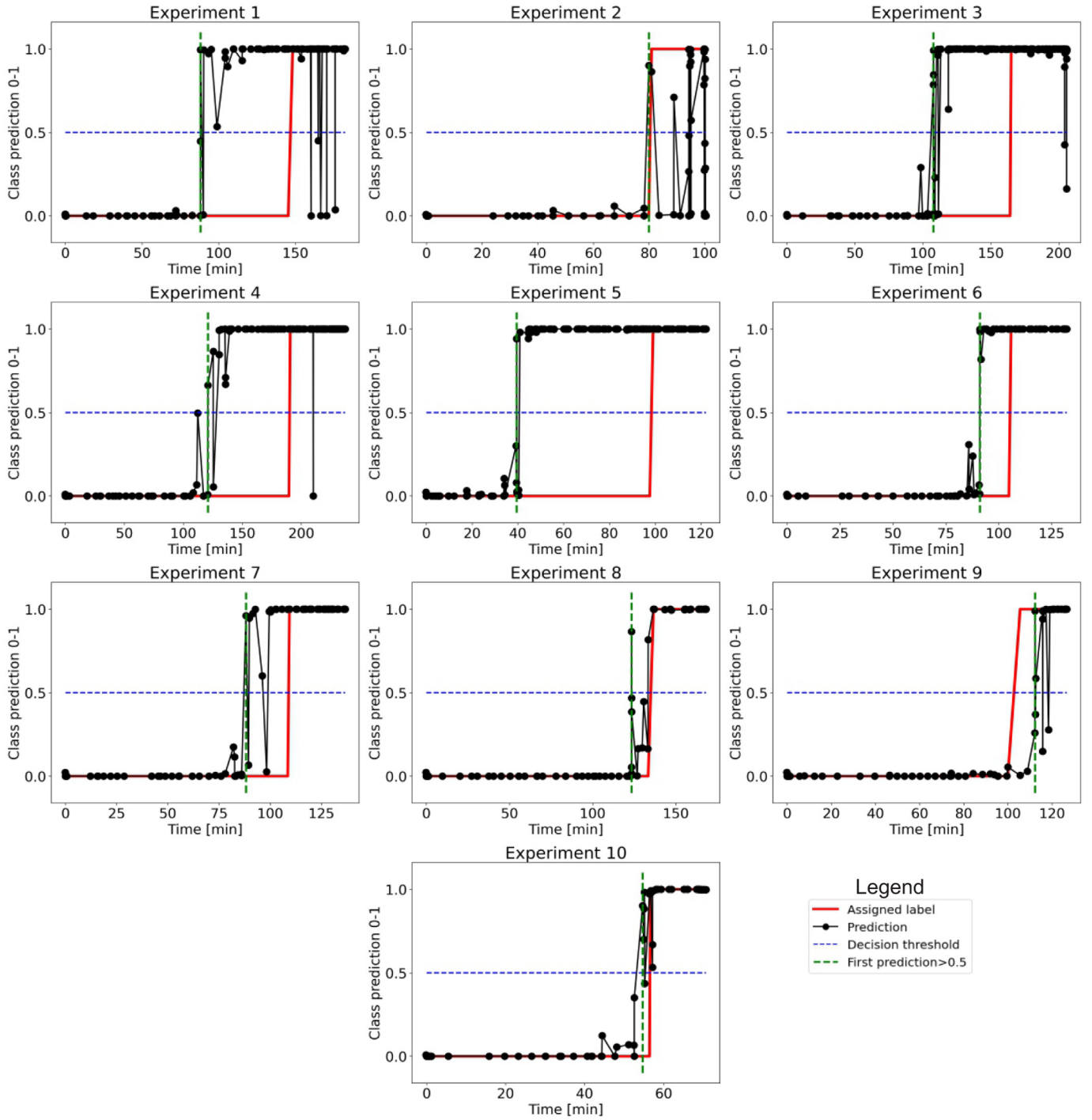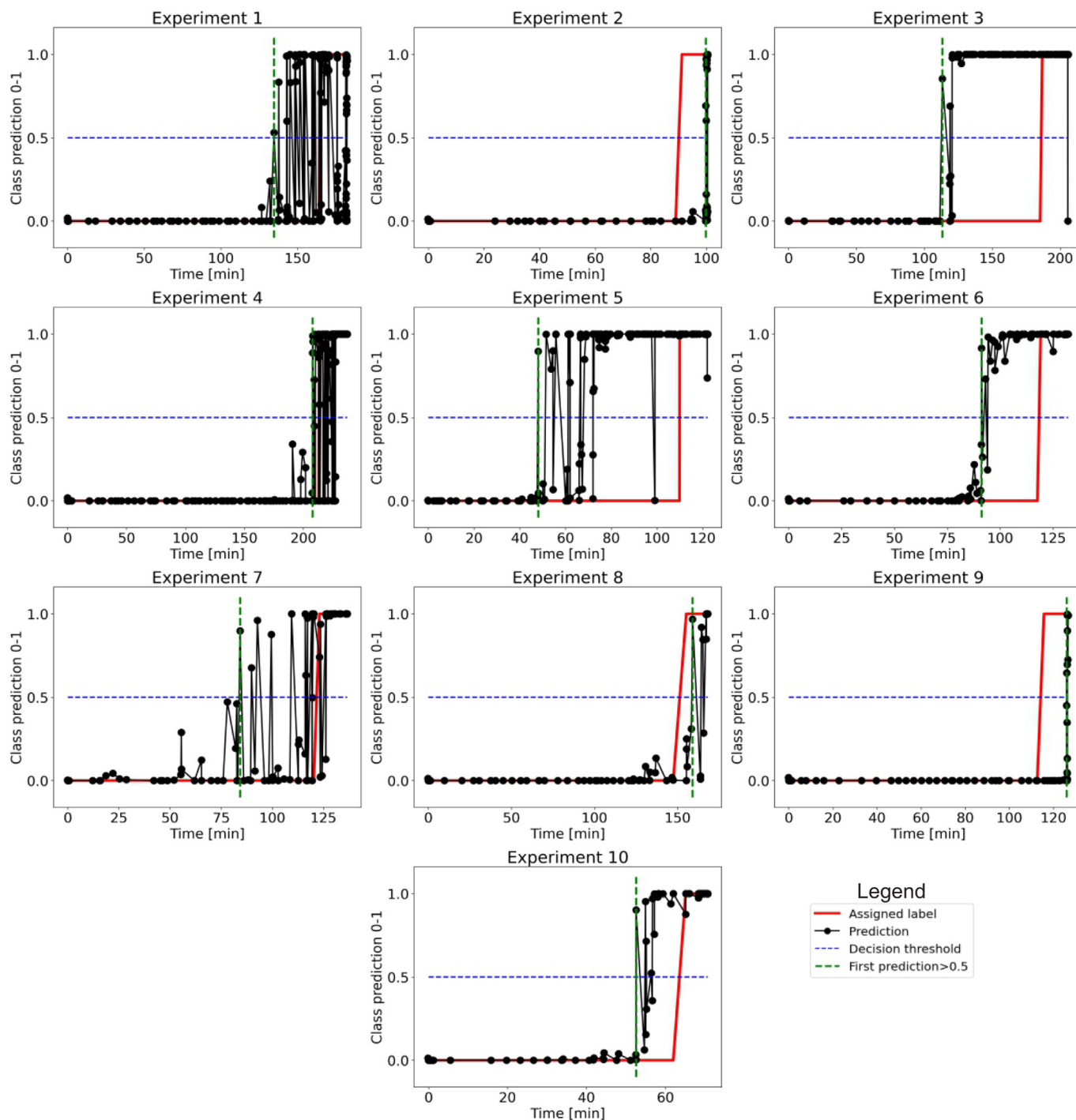
Fig. A.10. Results using a time threshold of 0.8.

Fig. A.11. Results using a time threshold of 0.9.

CRediT authorship contribution statement

Luis Orellana: Investigation, Writing – original draft, Software, Formal analysis. **Jorge Ardila-Rey:** Conceptualization, Methodology, Writing – review & editing, Supervision, Project administration. **Gonzalo Avaria:** Writing – review & editing, Formal analysis. **Sergio Davis:** Software, Formal analysis, Writing – review & editing.

Declaration of competing interest

Data availability

Acknowledgments

Appendix. Detailed results

See Figs. A.8–A.11.

References

33.04.01, CIGRE TF, 2000. Polluted insulators : A Review of Current Knowledge. CIGRE Tech. Brochure 158, 128–129, URL http://ci.nii.ac.jp/naid/10016820733/en/.

33.04.03, C., 1994. Insulator pollution monitoring. CIGRE Tech. Brochure.

Bezerra, J.M.d.B., Lima, A.M.N., Deep, G.S., da Costa, E.G., 2009. An evaluation of alternative techniques for monitoring insulator pollution. IEEE Trans. Power Deliv. 24 (4), 1773–1780. http://dx.doi.org/10.1109/TPWRD.2009.2016628.

Chandrasekar, S., Kalaivanan, C., Montanari, G.C., Cavallini, A., 2010. Partial discharge detection as a tool to infer pollution severity of polymeric insulators. IEEE Trans. Dielectrics Electr. Insul. 17 (1), 181–188. http://dx.doi.org/10.1109/TDEI.2010.5412016.

De Santos, H., Sanz Bobi, M.A., 2020. A Cumulative Pollution Index for the Estimation of the Leakage Current on Insulator Strings. IEEE Trans. Power Deliv. 35 (5), 2438–2446. http://dx.doi.org/10.1109/TPWRD.2020.2968556.

El-Hag, A., 2021. Application of Machine Learning in Outdoor Insulators Condition Monitoring and Diagnostics. IEEE Instrum. Meas. Mag. 24 (2), 101–108. http://dx.doi.org/10.1109/MIM.2021.9400959.

El-Kishky, H., Gorur, R.S., 1996. Electric field and energy computation on wet insulating surfaces. IEEE Trans. Dielectrics Electr. Insul. 3 (4), 587–593. http://dx.doi.org/10.1109/94.536739.

Ferreira, T.V., Germano, A.D., Silva, K.M., Costa, E.G., 2012. Ultra-sound and artificial intelligence applied to the diagnosis of insulations in the site. Gaodianya Jishu/High Voltage Eng. 38 (8), 1842–1847. http://dx.doi.org/10.3969/j.issn.1003-6520.2012.08.005.

He, L., Gorur, R.S., 2016a. Source strength impact analysis on insulator flashover under contaminated conditions. IEEE Trans. Dielectrics Electr. Insul. 23 (2), 1005–1011. http://dx.doi.org/10.1109/TDEI.2015.005264.

He, L., Gorur, R.S., 2016b. Source Strength Impact Analysis on Polymer Insulator Flashover under Contaminated Conditions and a Comparison with Porcelain. IEEE Trans. Dielectrics Electr. Insul. 23 (4), 2189–2195. http://dx.doi.org/10.1109/TDEI.2016.005770.

Hochreiter, S., Schmidhuber, J., 1997. Long Short-Term Memory. Neural Comput. 50 (9), 1735–1780. http://dx.doi.org/10.1162/neco.1997.9.8.1735.

IEC, 2014. Artificial Pollution Tests on High-Voltage Ceramic and Glass Insulators To Be Used on a.C. Systems. pp. 1–46.

James, G., Witten, D., Trevor, H., Tibshirani, R., 2013. An Introduction to Statistical Learning. Current Medicinal Chemistry. Springer US, http://dx.doi.org/10.2174/0929867003374372.

Jin, L., Ai, J., Han, S., Zhou, G., 2021. Probability Calculation of Pollution Flashover on Insulators and Analysis of Environmental Factors. IEEE Trans. Power Deliv. 36 (6), 3714–3723. http://dx.doi.org/10.1109/TPWRD.2020.3048750.

Jin, L., Ai, J., Tian, Z., Zhang, Y., 2017. Detection of polluted insulators using the information fusion of multispectral images. IEEE Trans. Dielectrics Electr. Insul. 24 (6), 3530–3538. http://dx.doi.org/10.1109/TDEI.2017.006516.

Jin, L., Zhang, D., 2015. Contamination grades recognition of ceramic insulators using fused features of infrared and ultraviolet images. Energies 8 (2), 837–858. http://dx.doi.org/10.3390/en8020837.

Kates-Harbeck, J., Svyatkovskiy, A., Tang, W., 2019. Predicting disruptive instabilities in controlled fusion plasmas through deep learning. Nature http://dx.doi.org/10.1038/s41586-019-1116-4.

Lecun, Y., Bengio, Y., Hinton, G., 2015. Deep learning. Nature 521 (7553), 436–444. http://dx.doi.org/10.1038/nature14539.

Liu, Y., Farzaneh, M., Du, B.X., 2016. Nonlinear characteristics of leakage current for flashover monitoring of ice-covered suspension insulators. IEEE Trans. Dielectrics Electr. Insul. 23 (3), 1242–1250. http://dx.doi.org/10.1109/TDEI.2015.005396.

Lu, S., Chai, H., Sahoo, A., Phung, B.T., 2020. Condition Monitoring based on Partial Discharge Diagnostics using Machine Learning Methods : A Comprehensive State-of-the-Art Review. IEEE Trans. Dielectrics Electr. Insul. In Press (6), http://dx.doi.org/10.1109/TDEI.2020.009070.

Mussina, D., Irmanova, A., Jamwal, P., Bagheri, M., 2020. Multi-modal Data Fusion using Deep Neural Network for Condition Monitoring of High Voltage Insulator. IEEE Access XX, 1. http://dx.doi.org/10.1109/access.2020.3027825.

Paula Santos Petri, L.D., Moutinho, E.A., Silva, R.P., Capelini, R.M., Salustiano, R., Figueiredo Ferraz, G.M., Wanderley Neto, E.T., Villibor, J.P., Pinto, S.S., 2020. A portable system for the evaluation of the degree of pollution of transmission line insulators. Energies 13 (24), 6625. http://dx.doi.org/10.3390/en13246625.

Polisetty, S., El-Hag, A., Jayram, S., 2019. Classification of common discharges in outdoor insulation using acoustic signals and artificial neural network. High Voltage 4 (4), 333–338. http://dx.doi.org/10.1049/hve.2019.0113.

Reddy, B.S., Nagabhushana, G.R., 2003. Study of Temperature Distribution Along an Artificially Polluted Insulator String. Plasma Sci. Technol. 5 (2), 1715–1720. http://dx.doi.org/10.1088/1009-0630/5/2/006.

Reid, A.J., Judd, M.D., Duncan, G., 2012. Simultaneous measurement of partial discharge using TEV, IEC60270 and UHF techniques. In: Conference Record of IEEE International Symposium on Electrical Insulation. pp. 439–442. http://dx.doi.org/10.1109/ELINSL.2012.6251506.

Richards, C.S., Banner, C.L., Butler-Purry, K.L., Don Russell, B., 2003. Electrical behavior of contaminated distribution insulators exposed to natural wetting. IEEE Trans. Power Deliv. 18 (2), 551–558. http://dx.doi.org/10.1109/TPWRD.2003.809682.

Robles, G., Albarracin, R., Vazquez-Roy, J.L., Rajo-Iglesias, E., Martinez-Tarifa, J.M., Rojas-Moreno, M.V., Sanchez-Fernandez, M., Ardila-Rey, J., 2013. On the use of Vivaldi antennas in the detection of partial discharges. In: Proceedings of IEEE International Conference on Solid Dielectrics, ICSD. pp. 302–305. http://dx.doi.org/10.1109/ICSD.2013.6619887.

Shurrab, I.Y., El-Hag, A.H., Assaleh, K., Ghunem, R.A., Jayaram, S., 2013. RF-based monitoring and classification of partial discharge on wet silicone rubber surface. IEEE Trans. Dielectrics Electr. Insul. 20 (6), 2188–2194. http://dx.doi.org/10.1109/TDEI.2013.6678869.

Wilkins, R., 1969. Flashover voltage of high-voltage insulators with uniform surface-pollution films. Proc. Inst. Electr. Eng. 116 (3), 457. http://dx.doi.org/10.1049/piee.1969.0093.

Zhao, C., Mei, H., Zhu, M., Dai, H., Wang, L., Zhou, Z., 2015. Development of contamination flashover pre-warning system and analysis of operating experience. IEEE Trans. Dielectrics Electr. Insul. 22 (4), 2234–2241. http://dx.doi.org/10.1109/TDEI.2015.004472.